Hindawi Publishing Corporation
Shock and Vibration
Volume 2016, Article ID 5414361, 11 pages
http://dx.doi.org/10.1155/2016/5414361

Research Article

Correlation Coefficient of Simplified Neutrosophic Sets for Bearing Fault Diagnosis

Lilian Shi

Department of Electrical and Information Engineering, Shaoxing University, 508 Huancheng West Road, Shaoxing, Zhejiang Province 312000, China

Correspondence should be addressed to Lilian Shi; sllian@sina.com

Received 18 May 2016; Revised 26 September 2016; Accepted 3 October 2016

Academic Editor: Mariano Artés

Copyright © 2016 Lilian Shi. This is an open access article distributed under the Creative Commons Attribution License, which permits unrestricted use, distribution, and reproduction in any medium, provided the original work is properly cited.

In order to process the vagueness in vibration fault diagnosis of rolling bearing, a new correlation coefficient of simplified neutrosophic sets (SNSs) is proposed. Vibration signals of rolling bearings are acquired by an acceleration sensor, and a morphological filter is used to reduce the noise effect. Wavelet packet is applied to decompose the vibration signals into eight subfrequency bands, and the eigenvectors associated with energy eigenvalue of each frequency are extracted for fault features. The SNSs of each fault types are established according to energy eigenvectors. Finally, a correlation coefficient of two SNSs is proposed to diagnose the bearing fault types. The experimental results show that the proposed method can effectively diagnose the bearing faults.

1. Introduction

A rolling bearing is an important rotating part in a mechanical equipment, and its quality decides the operation performance of the equipment. A faulty bearing may cause the whole equipment to operate abnormally. Bearing faults must be effectively diagnosed to avoid catastrophic mechanical failures and significant economic losses.

The vibration signals of rolling bearings often indicate some fault information. When the fault occurs in rotating bearings, different characteristic frequencies of vibration signals can be generated periodically [1]. Actually, for the original vibration signals, many useful fault features are usually hidden in noise, and the relationship between fault symptoms and causations is very complex, so it is difficult to make accurate and quantitative analysis for fault types. In recent years, many studies have been devoted to the fault diagnosis of rolling bearing. There are two critical issues for diagnosing bearing faults from vibration signals. One issue is how to extract fault features from vibration signals. Another one is how to analyze fault features and recognize fault types according to these features.

In order to extract useful fault features from vibration signals, many techniques such as time domain, frequency domain, and time-frequency domain methods are extensively investigated [2]. In the time domain method, key parameters can be extracted directly from the original vibration signals, such as root mean square (RMS), crest factor, peak, and probability density function [3]. In addition, time domain signals can be transformed into frequency domain by Fourier transform. However, Fourier analysis may cause information loss during the transformation, particularly for nonstationary signals. The vibration of a rolling bearing is typically nonstationary, so it is difficult to extract accurate and complete fault features when adopting the traditional analysis only in the time or frequency domain. In time-frequency domain, the wavelet can reveal more complete information for nonstationary signals [4]. Many research results show that a wavelet packet is an effective tool to extract features from vibration signals for bearing fault diagnosis [5–8].

The next key issue is to recognize fault types of bearings according to the extracted fault features from vibration signals. To solve this problem, various approaches such as expert systems [9, 10], neural networks [3, 11, 12], and fuzzy approaches [13–15] have been developed for fault diagnosis over the past few years. Fuzzy theory has attracted increasing attention in bearing fault diagnosis, and many researches

show that fuzzy theory is an effective tool to diagnose bearing faults.

Fuzzy sets (FSs) theory was proposed by Zadeh (1965) for handling uncertain information using single membership degree function [16]. The fuzzy sets were extended to intuitionistic fuzzy sets (IFSs) [17] and interval valued intuitionistic fuzzy sets (IVIFSs) [18] by using membership degree function, non-membership degree function, and degree function of hesitation simultaneously. FSs, IFSs, and IVIFSs have been widely applied in various fields. However, FSs, IFSs, and IVIFSs cannot deal with some types of uncertainties such as the indeterminate information and inconsistent information in real physical problems. Furthermore, Smarandache [19] proposed neutrosophy theory from philosophical point of view. Neutrosophic sets (NSs) are characterized by a truth-membership function, an indeterminacy-membership function, and a falsity-membership function. The functions of NSs take the value from real standard or nonstandard subsets of $]^{-}0, 1^{+}[$ [19], and NSs are difficult to be applied in engineering areas. For the real engineering applications, neutrosophic sets (NSs) can be described as simplified neutrosophic sets (SNSs) [20] with the normal standard real unit interval $[0, 1]$. One major advantage of SNSs is the ability to perform analysis problems involving imprecise, undetermined, and inconsistent data. Recently, SNSs have been applied in many different fuzzy problems, such as medical diagnosis problems [21, 22], decision making problems [20, 23], and image processing [24].

For vibrational fault diagnosis of rolling bearing, there is no direct accurate and quantitative relationship between fault vibration characteristics and fault types. Therefore, the fault-diagnosis process has certain vagueness. This paper mainly focuses on the fault diagnosis of rolling bearings based on vibration signals and SNSs. In this work, a morphological filter and wavelet packet decomposition are applied to preprocess the original vibration signals, and the SNSs of each fault type will be established according to energy eigenvectors. The fault types will be diagnosed using a new correlation coefficient of SNSs.

The rest of the paper is organized as follows. Section 2 gives the experimental system. Section 3 gives the data preprocessing techniques including morphological opening-closing operation and wavelet packet decomposition. In Section 4, some basic concepts of SNSs and a new correlation coefficient are introduced firstly, and then the fault-diagnosis method is presented based on SNSs. Conclusions of this work are summarized in Section 5.

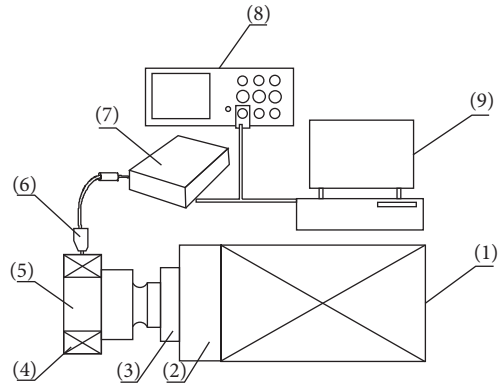

Figure 1: Diagram of experimental system. (1) Motor, (2) driver, (3) principal axis, (4) bearing, (5) core axes, (6) acceleration sensor, (7) acquisition data card, (8) oscilloscope, and (9) computer.

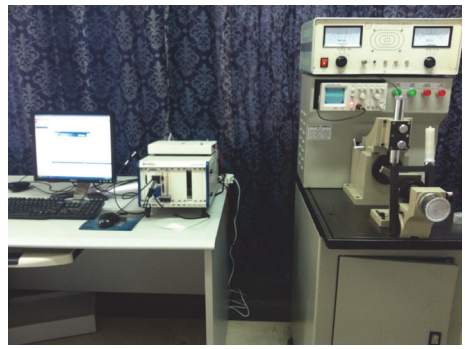

Figure 2: Experimental device.

Table 1: Bearing parameters.

Parameters	Values (mm)
Outer race diameter	35
Inner race diameter	15
Ball diameter d	7.5
Thickness	11
Number of balls	7
Pitch diameter D	25
Contact angle α	0

2. Experimental Setup

This study was carried out with the experimental apparatus shown in Figure 1. The principal axis is driven by an AC motor, and the vibration signals of bearings are acquired by an acceleration sensor and a data acquiring card NI USB-6251. The vibration signals will be processed using a computer and displayed by an oscilloscope. Some vibration signals are acquired by the experimental device of Jiliang University in China [25], shown in Figure 2. In this experiment, the type of bearings is NSK 6202 deep groove ball bearing whose specifications are listed in Table 1.

In order to diagnose the fault of bearings, four types of bearings are used: healthy, outer race fault, inner race fault, and ball fault bearings. The core axis is driven at the rotational speed of 25 Hz. NI Labview Signal Express will be applied for data acquisition with 10 KHz sampling frequency and 0.2 s sample time.

When a fault exists in a bearing, vibration impulses will happen at a specific frequency. Theoretically, when a bearing

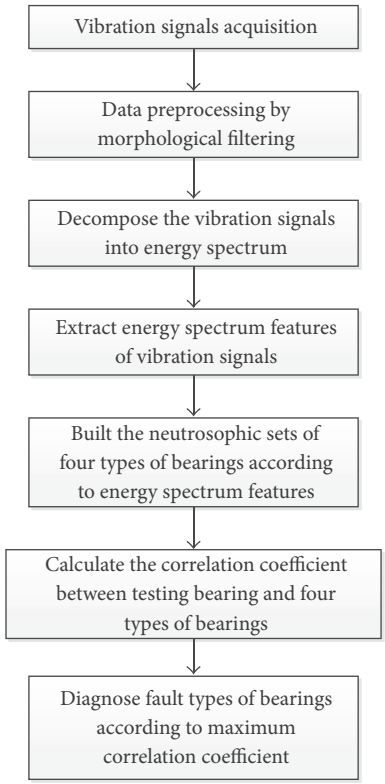

Figure 3: Block diagram of diagnosis for fault bearing using neutrosophic sets.

rotates at a constant speed, the fault frequencies can be calculated by the following [26]:

$$F_O = \frac{N_B}{2}\left(1 - \frac{d}{D}\cdot\cos\alpha\right)\cdot F_r,$$
$$F_I = \frac{N_B}{2}\left(1 + \frac{d}{D}\cdot\cos\alpha\right)\cdot F_r, \quad (1)$$
$$F_B = \frac{D}{d}\left[1 - \left(\frac{d}{D}\cdot\cos\alpha\right)^2\right]\cdot F_r,$$

where d is the diameter of the rolling elements, D is the pitch diameter, F_r is the rotational speed of the shaft, N_B is the number of rolling elements, and F_O, F_I, and F_B represent the fault frequencies of outer race fault, inner race fault, and ball fault of a bearing, respectively.

According to (1), we can calculate the fault frequencies $F_O = 61.25$ Hz, $F_I = 113.75$ Hz, and $F_B = 75.83$ Hz in this experiment.

3. Vibration Signal Data Preprocessing

The framework of diagnosing process is shown in Figure 3.

The original vibration signals of bearings are usually ridden with noise. It is difficult to extract the fault features directly from original vibration signals. In order to remove the strong noises and detect the effective signals for bearing faults diagnosis, data processing algorithms are necessary to be performed. In this experiment, a morphological filter is used to remove high frequencies noise from the original vibration signals firstly, and then wavelet packet is applied to decompose the signals into the individual frequencies.

3.1. Morphological Filter. A morphological filter is a nonlinear signal processing and analysis tool in time domain, and it can be composed of several morphological operations [27]. The basic morphological operators include dilation, erosion, opening, and closing. Assume that $x(n)$ and a structural element $y(n)$ are discrete signals defined in $X = \{0, 1, \ldots, N-1\}$ and $B = \{0, 1, \ldots, M-1\}$, respectively, and $N \geq M$, the four basic operators of $x(n)$ on $y(n)$, are defined as follows:

Dilation

$$x \oplus y = \max_{m=0,1,\ldots,M-1}\{x(n+m) + y(m)\}, \quad (n = 0, 1, \ldots, N+M) \quad (2)$$

Erosion

$$x \ominus y = \min_{m=0,1,\ldots,M-1}\{x(n+m) - y(m)\}, \quad (n = 0, 1, \ldots, N+M) \quad (3)$$

Opening

$$x \circ y = (x \ominus y \oplus y) \quad (4)$$

Closing

$$x \bullet y = (x \oplus y \ominus y) \quad (5)$$

Morphological opening-closing filter as follows:

$$F_{oc} = (x \circ y \bullet y) \quad (6)$$

In this experiment, the morphological opening-closing filter F_{oc} was used to remove the strong noises.

Figures 4–6 show the signals of rolling element bearings with outer race, inner race, and ball fault, respectively [25]. In these figures, the fault signals have distinguishing peak value features at the fault frequencies. The results in Figures 4–6 indicate that morphological filter is an effective denoising technique for vibration signals of ball bearings.

3.2. Wavelet Packet Decomposition. According to the structure of wavelet decomposition, the input vibration signal can be decomposed into low-frequency and high-frequency parts for each step. The selection of a suitable level for the hierarchy depends on the signal, experience, and actual needs [4, 7]. The wavelet packet was applied to decompose the vibration signals into eight subfrequency bands in the practical application [2, 6]. Based on review of earlier researcher, in this work, 3-level wavelet packet decomposition is considered for bearing fault diagnosis, and experimental results show that the bearing fault feature can be extracted effectively from the decomposed signals.

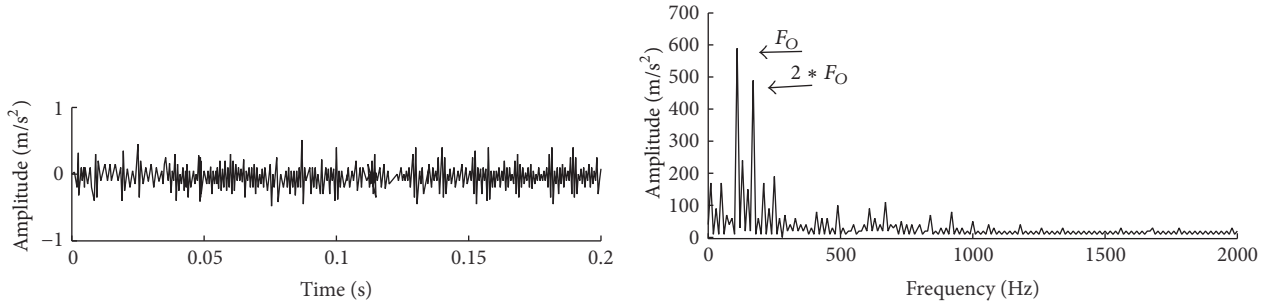

(a) Original vibration in time domain

(b) Fast Fourier transform after morphological filter

Figure 4: Signals of rolling bearing in outer race fault.

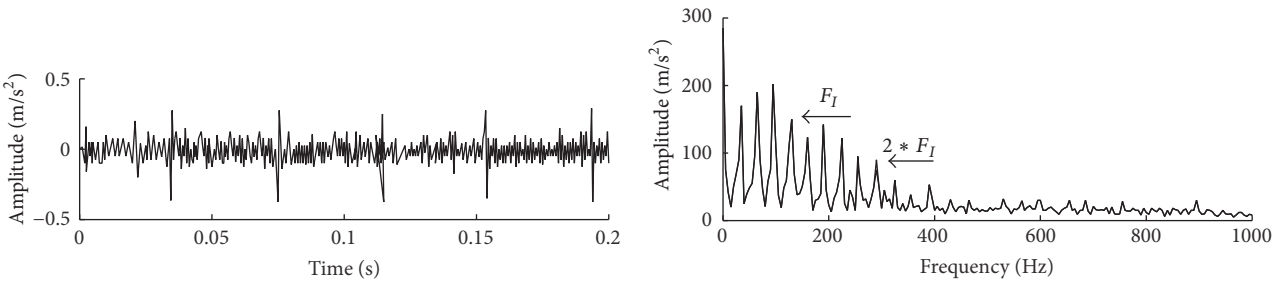

(a) Original vibration in time domain

(b) Fast Fourier transform after morphological filter

Figure 5: Signals of rolling bearing in inner race fault.

In this experiment, the vibration signals of bearing are preprocessed firstly by a morphological filter and then are decomposed using 3-level wavelet packet.

Assume that $x(t)$ is a vibration signal; $L(\cdot)$ and $H(\cdot)$ are quadrature mirror filters, representing low-pass and high-pass wavelet filters, respectively. These filters associate with the scaling function and wavelet function and satisfy the condition $H(n) = (-1)^n L(1-n)$. Then, the signal $x(t)$ can be decomposed into a set of high- and low-frequency components by the following recursive relationships:

$$x_{j,2k} = \sum_n L(n) \cdot x_{j-1,k},$$
$$x_{j,2k+1} = \sum_n H(n) \cdot x_{j-1,k}, \tag{7}$$

where $x_{j,2k}$ denotes the wavelet coefficients at the jth level and $2k$th subband.

The diagram of 3-level wavelet packet decomposition is shown in Figure 7. In Figure 7, the frequency intervals of each band can be computed by $((k-1)f_s/2^4, kf_s/2^4]$, where f_s is sampling frequency. In this work, $f_s = 10\,\text{kHz}$ and $f_s/2^4 = 625\,\text{Hz}$. The frequency intervals are given in Table 2.

The vibration signal $x(t)$ can be expressed as follows:

$$x(t) = \sum_{k=0}^{2^3-1} x_{3,k}(t), \quad k = 0, 1, \ldots, 7, \tag{8}$$

where k represents eight subfrequency bands and $x_{3,k}(t)$ is the wavelet coefficient at the 3-level and kth subfrequency band.

Table 2: Frequency intervals of eight subfrequency bands.

Signals	Frequency (Hz)
$x_{3,0}$	(0, 625]
$x_{3,1}$	(625, 1250]
$x_{3,2}$	(1250, 1875]
$x_{3,3}$	(1875, 2500]
$x_{3,4}$	(2500, 3125]
$x_{3,5}$	(3125, 3750]
$x_{3,6}$	(3750, 4375]
$x_{3,7}$	(4375, 5000]

After the decomposition, the energy in each subfrequency band can be defined as

$$E_3^k = \int |x_{3,k}(t)|^2 dt = \sum_{i=0}^{N} |x_{3,k}(i)|^2, \quad k = 0, 1, \ldots, 7, \tag{9}$$

where $x_{3,k}(i)$ is the ith discrete point amplitude of wavelet coefficient $(x_{3,k}(t))$ and N is its discrete point number in each subfrequency.

The faults of rolling bearings will greatly influence the wavelet packet energy of vibration signals, so it is very useful to extract the energy eigenvalue for diagnosing bearing faults. In this experiment, an eigenvector based on energy eigenvalue of each frequency can be constructed as follows:

$$T = \left\{E_3^0, E_3^1, E_3^2, E_3^3, E_3^4, E_3^5, E_3^6, E_3^7\right\}. \tag{10}$$

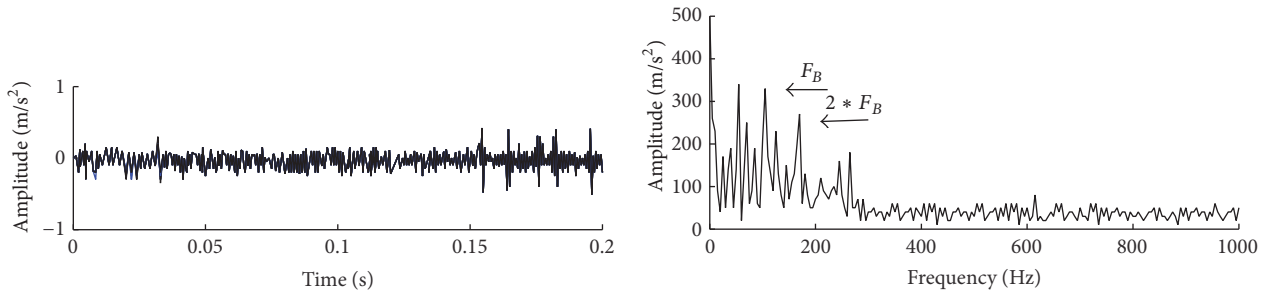

(a) Original vibration in time domain

(b) Fast Fourier transform after morphological filter

Figure 6: Signals of rolling bearing in ball fault.

Table 3: Energy interval ranges at the eight subfrequency bands.

Fault types	Energy in each frequency band							
	E_3^{*0}	E_3^{*1}	E_3^{*2}	E_3^{*3}	E_3^{*4}	E_3^{*5}	E_3^{*6}	E_3^{*7}
A_1 (healthy)	[0.76, 0.80]	[0.95, 1.00]	[0.11, 0.15]	[0.64, 0.71]	[0.04, 0.06]	[0.00, 0.02]	[0.01, 0.05]	[0.00, 0.03]
A_2 (outer race fault)	[1.00, 1.00]	[0.24, 0.39]	[0.02, 0.03]	[0.13, 0.22]	[0.00, 0.01]	[0.00, 0.01]	[0.01, 0.01]	[0.01, 0.01]
A_3 (ball fault)	[0.82, 0.93]	[1.00, 1.00]	[0.11, 0.16]	[0.65, 0.74]	[0.06, 0.08]	[0.00, 0.04]	[0.02, 0.06]	[0.00, 0.01]
A_4 (inner race fault)	[1.00, 1.00]	[0.49, 0.55]	[0.06, 0.10]	[0.20, 0.24]	[0.00, 0.00]	[0.02, 0.03]	[0.03, 0.05]	[0.03, 0.06]

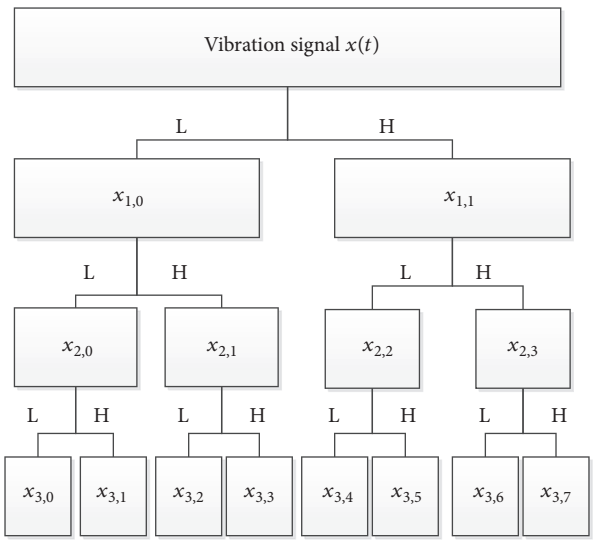

Figure 7: Diagram of 3-level wavelet packet decomposition (L: low-pass filter, H: high-pass filter).

Furthermore, assume that $E_{3\max}$ is the maximum value of the energy eigenvalue in the 3-level subfrequency band, and then the eigenvalues can be normalized as follows:

$$E_3^{*k} = \frac{E_3^k}{E_{3\max}}, \quad k = 0, 1, \ldots, 7. \tag{11}$$

By the above normalization, the energy eigenvalue of the wavelet packet energy of vibration signals was bounded to [0, 1], and then the normalized eigenvector can be described as follows:

$$T^* = \left\{E_3^{*0}, E_3^{*1}, E_3^{*2}, E_3^{*3}, E_3^{*4}, E_3^{*5}, E_3^{*6}, E_3^{*7}\right\}. \tag{12}$$

The normalized energy eigenvalues of vibration signals are shown in Figure 8.

For diffident type faults of bearing, the eigenvalue of the wavelet packet energy has the distinguishing distribution at the individual subfrequency band. According to a lot of experimentation and data comparison, we extract the lower bound and upper bound of the energy eigenvalues for typical faults of bearing and establish the energy interval ranges as shown in Table 3, and the energy interval ranges can be used to diagnose fault types of rolling bearings in the next step.

4. Fault Diagnosis of Rolling Bearing Based on SNSs

In this section, we briefly introduce basic concepts of simplified neutrosophic sets (SNSs) and propose a new correlation coefficient of two SNSs, which will be needed in the following analysis. Then, we establish the fault SNSs of bearings according to energy features. Finally, we present the method for fault diagnosis of rolling bearing according to the correlation coefficient of SNSs.

4.1. Simplified Neutrosophic Sets (SNSs)

Definition 1 (see [19]). Let U be a universe of discourse; then, the neutrosophic set (NS) A is defined by

$$A = \left\{\left\langle x, T_A(x), I_A(x), F_A(x)\right\rangle, \ x \in U\right\}, \tag{13}$$

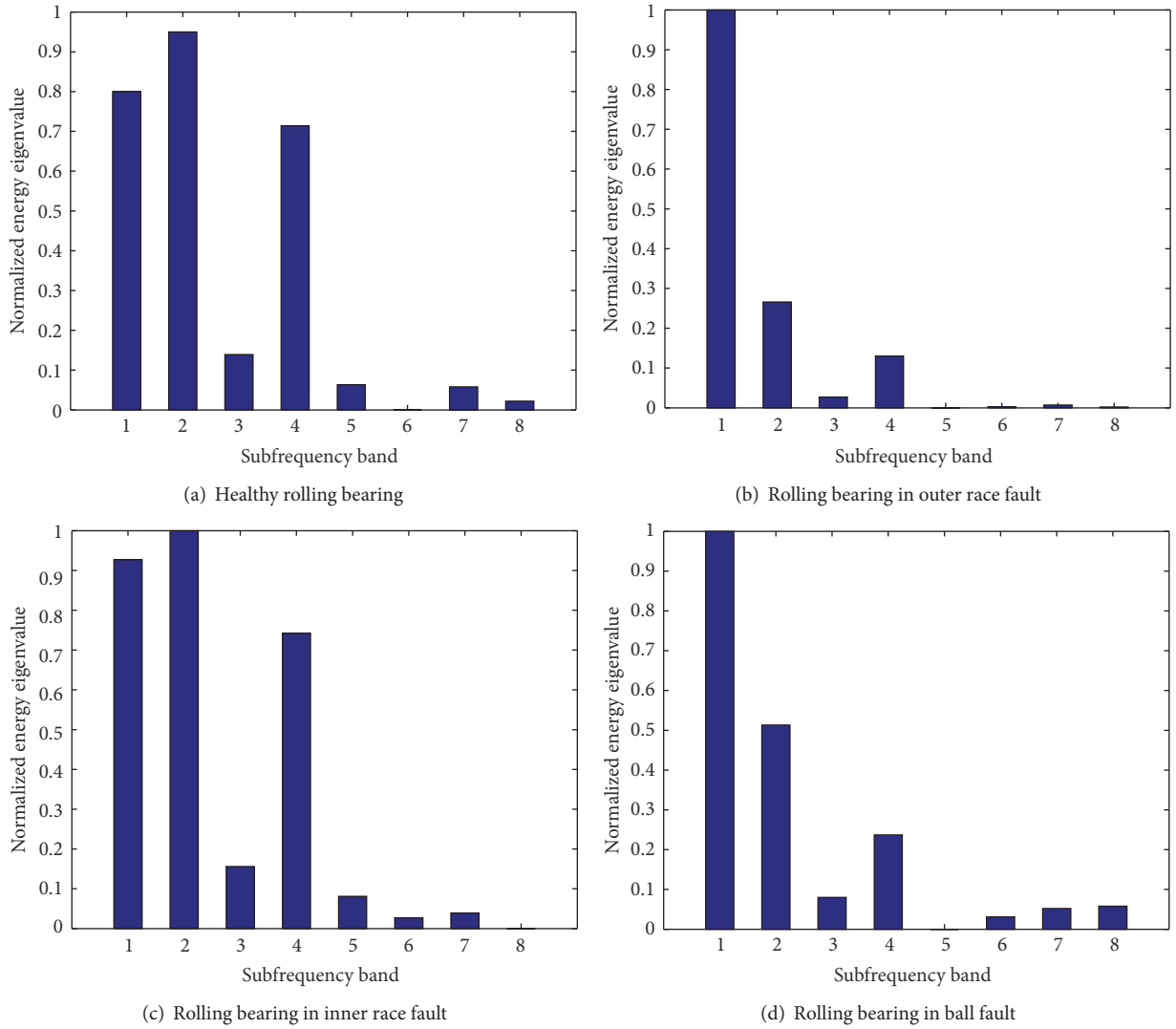

Figure 8: Energy histogram of rolling bearing.

where the functions $T_A(x)$, $I_A(x)$, and $F_A(x)$ represent a truth-membership function, an indeterminacy-membership function, and a falsity-membership function of the element $x \in U$ to the set A, respectively, with the conditions $T_A(x), I_A(x), F_A(x)\colon U \to]^-0, 1^+[$ and $^-0 \leq \sup T_A(x) + \sup I_A(x) + \sup F_A(x_i) \leq 3^+$.

The above concept of a neutrosophic set (NS) is presented from philosophical point of view, and it takes the value from real standard or nonstandard subsets of $]^-0, 1^+[$. It will be difficult to apply $]^-0, 1^+[$ in scientific and engineering areas. For the real applications, a simplified neutrosophic set (SNS) is introduced by Ye [20] as the following definition.

Definition 2 (see [20]). Let U be a space of points (objects) with generic elements in U denoted by x. A simplified neutrosophic set (SNS) A in U is characterized by a truth-membership function $T_A(x)$, an indeterminacy-membership function $I_A(x)$, and a falsity-membership function $F_A(x)$. For each point x in U, $T_A(x)$, $I_A(x)$, and $F_A(x)$ are singleton subintervals/subsets in the real standard $[0, 1]$, such that $T_A(x), I_A(x), F_A(x) \in [0, 1]$. Then, a simplified neutrosophic set (SNS) is denoted by

$$A = \{\langle x, T_A(x), I_A(x), F_A(x)\rangle \mid x \in U\}. \quad (14)$$

Obviously, a simplified neutrosophic set (SNS) is a subclass of the neutrosophic set (NS) and satisfies the conditions $T_A(x), I_A(x), F_A(x)\colon U \to [0, 1]$ and $0 \leq T_A(x) + I_A(x) + F_A(x) \leq 3$.

4.2. Correlation Coefficient for SNSs. Correlation coefficient is an important tool for determining the correlation degree between fuzzy sets. Therefore, a new correlation coefficient of two SNSs is proposed by the following definition.

Definition 3. Assume that there are two SNSs $A = \{\langle x_i, T_A(x_i), I_A(x_i), F_A(x_i)\rangle \mid x_i \in U\}$ and $B = \{\langle x_i, T_B(x_i), I_B(x_i), F_B(x_i)\rangle \mid x_i \in U\}$ in the universe of discourse $U = \{x_1,$

$x_2, \ldots, x_n\}$, $x_i \in U$. A correlation coefficient between SNSs is defined as follows:

$$M_{\mathrm{SNS}}(A,B) = \frac{1}{n}\sum_{i=1}^{n} \frac{\min\left[T_A(x_i), T_B(x_i)\right] + \min\left[I_A(x_i), I_B(x_i)\right] + \min\left[F_A(x_i), F_B(x_i)\right]}{\sqrt{T_A(x_i)\,T_B(x_i)} + \sqrt{I_A(x_i)\,I_B(x_i)} + \sqrt{F_A(x_i)\,F_B(x_i)}}, \tag{15}$$

where the symbol "min" is the minimum operation.

According to the above definition, the correlation coefficient of SNSs A and B satisfies the following properties:

(P_1) $0 \le M_{\mathrm{SNS}}(A,B) \le 1$.

(P_2) $M_{\mathrm{SNS}}(A,B) = M_{\mathrm{SNS}}(B,A)$.

(P_3) $M_{\mathrm{SNS}}(A,B) = 1$ if and only if $A = B$.

If we consider the weights of x_i, a weighted correlation coefficient between SNSs A and B is proposed as follows:

$$M_{\mathrm{SNS}}(A,B) = \sum_{i=1}^{n} w_i \frac{\min\left[T_A(x_i), T_B(x_i)\right] + \min\left[I_A(x_i), I_B(x_i)\right] + \min\left[F_A(x_i), F_B(x_i)\right]}{\sqrt{T_A(x_i)\,T_B(x_i)} + \sqrt{I_A(x_i)\,I_B(x_i)} + \sqrt{F_A(x_i)\,F_B(x_i)}}, \tag{16}$$

where $w_i \in [0,1]$ and $\sum_{i=1}^{n} w_i = 1$ for $i = 1, 2, \ldots, n$.

4.3. Bearings Neutrosophic Sets Models Based on Energy Eigenvectors. The SNSs models of rolling bearings can be built according to the energy intervals of the eight subfrequency bands as shown in Table 3.

Assume that a set of bearing faults is $A = \{A_1$ (healthy), A_2 (outer race fault), A_3 (ball fault), A_4 (inner race fault)$\}$, and a set of energy eigenvector is $E = \{e_1(E_3^{*0}), e_2(E_3^{*1}), e_3(E_3^{*2}), e_4(E_3^{*3}), e_5(E_3^{*4}), e_6(E_3^{*5}), e_7(E_3^{*6}), e_8(E_3^{*7})\}$. In Table 3, let $T_{Ak}(e_i)$ and $U_{Ak}(e_i)$ $(k = 1,2,3,4;\ i = 1,2,\ldots,8)$ be the lower bound and upper bound of the characteristic value e_i for A_k, respectively; then, the characteristic intervals of rolling bearing can be represented by

$$\begin{aligned} A_k = \{&(e_1, [T_{Ak}(x_1), U_{Ak}(e_1)]),\\ &(e_2, [T_{Ak}(e_2), U_{Ak}(e_2)]), (e_3, [T_{Ak}(e_3), U_{Ak}(e_3)]),\\ &(e_4, [T_{Ak}(e_4), U_{Ak}(e_4)]), (e_5, [T_{Ak}(e_5), U_{Ak}(e_5)]),\\ &(e_6, [T_{Ak}(e_6), U_{Ak}(e_6)]), (e_7, [T_{Ak}(e_7), U_{Ak}(e_7)]),\\ &(e_8, [T_{Ak}(e_8), U_{Ak}(e_8)])\}, \quad (k = 1,2,3,4) \end{aligned} \tag{17}$$

Let $U_{Ak}(e_i) = 1 - F_{Ak}(e_i)$ and $I_{Ak}(e_i) = U_{Ak}(e_i) - T_{Ak}(e_i)$, for $k = 1, \ldots, 4$ and $i = 1, \ldots, 8$. If $U_{Ak}(e_i) - T_{Ak}(e_i) \le 0.01$, then let $I_{Ak}(e_i) = 0.01$. In this case, the sets A_k can be extended to simplified neutrosophic sets (SNSs) and can be rewritten as

$$\begin{aligned} A_k = \{&\langle e_1, T_{Ak}(e_1), I_{Ak}(e_1), F_{Ak}(e_1)\rangle,\\ &\langle e_2, T_{Ak}(e_2), I_{Ak}(e_2), F_{Ak}(e_2)\rangle,\\ &\langle e_3, T_{Ak}(e_3), I_{Ak}(e_3), F_{Ak}(e_3)\rangle,\\ &\langle e_4, T_{Ak}(e_4), I_{Ak}(e_4), F_{Ak}(e_4)\rangle,\\ &\langle e_5, T_{Ak}(e_5), I_{Ak}(e_5), F_{Ak}(e_5)\rangle,\\ &\langle e_6, T_{Ak}(e_6), I_{Ak}(e_6), F_{Ak}(e_6)\rangle,\\ &\langle e_7, T_{Ak}(e_7), I_{Ak}(e_7), F_{Ak}(e_7)\rangle,\\ &\langle e_8, T_{Ak}(e_8), I_{Ak}(e_8), F_{Ak}(e_8)\rangle\}, \end{aligned} \tag{18}$$

where $T_{Ak}(e_i)$: $U \to [0,1]$, $I_{Ak}(e_i)$: $U \to [0,1]$, $F_{Ak}(e_i)$: $U \to [0,1]$, and $0 \ge T_{Ak}(e_i) + I_{Ak}(e_i) + F_{Ak}(e_i) \le 3$, for $k = 1, \ldots, 4$ and $i = 1, \ldots, 8$.

According to the definition of neutrosophic sets, the numbers $T_{Ak}(e_i)$, $I_{Ak}(e_i)$, and $F_{Ak}(e_i)$ represent a truth-membership, an indeterminacy-membership, and a falsity-membership, respectively. The neutrosophic sets of bearing fault types are shown in Table 4. Here, A_1, A_2, A_3, and A_4 are healthy, outer race fault, ball fault, and inner race fault bearings, respectively.

4.4. Rolling Bearing Fault Diagnosis Using Correlation Coefficient. In this section, we apply the correlation coefficient of SNSs to diagnose rolling bearing faults. Assume that A_k $(k = 1,2,3,4)$ are SNSs models of rolling bearing faults and A_t is a testing rolling bearing signal expressed by a SNS. Then we can calculate the correlation coefficient value $M_{\mathrm{SNS}}(A_k, A_t)$ $(k = 1,2,3,4)$ using (16). Finally, the fault-diagnosis order of the fault-testing sample can be ranked according to the correlation coefficient value, and the proper diagnosis A_{k^*} for the bearing fault A_t is derived by

$$k^* = \arg\max_{1 \le k \le 4} \left\{M_{\mathrm{SNS}}(A_k, A_t)\right\}, \tag{19}$$

This paper considers the same importance of the energy values in each frequency band; therefore, the weights of w_i $(i = 1,2,\ldots,8)$ are $w_i = 1/8$.

Table 4: Energy values of bearing fault types represented by the form of SNS.

Fault types	Energy in each frequency band							
	E_3^{*0}	E_3^{*1}	E_3^{*2}	E_3^{*3}	E_3^{*4}	E_3^{*5}	E_3^{*6}	E_3^{*7}
A_1	$\langle e_1, 0.76, 0.14, 0.20\rangle$	$\langle e_2, 0.95, 0.05, 0.00\rangle$	$\langle e_3, 0.11, 0.04, 0.85\rangle$	$\langle e_4, 0.64, 0.07, 0.29\rangle$	$\langle e_5, 0.04, 0.02, 0.94\rangle$	$\langle e_6, 0.00, 0.02, 0.98\rangle$	$\langle e_7, 0.01, 0.05, 0.95\rangle$	$\langle e_8, 0.00, 0.03, 0.97\rangle$
A_2	$\langle e_1, 1.00, 0.01, 0.00\rangle$	$\langle e_2, 0.24, 0.15, 0.61\rangle$	$\langle e_3, 0.02, 0.01, 0.97\rangle$	$\langle e_4, 0.13, 0.09, 0.78\rangle$	$\langle e_5, 0.00, 0.01, 1.00\rangle$	$\langle e_6, 0.00, 0.01, 0.99\rangle$	$\langle e_7, 0.01, 0.01, 0.99\rangle$	$\langle e_8, 0.01, 0.01, 0.99\rangle$
A_3	$\langle e_1, 0.82, 0.11, 0.07\rangle$	$\langle e_2, 1.00, 0.01, 0.00\rangle$	$\langle e_3, 0.11, 0.05, 0.84\rangle$	$\langle e_4, 0.65, 0.10, 0.25\rangle$	$\langle e_5, 0.06, 0.03, 0.92\rangle$	$\langle e_6, 0.00, 0.04, 0.96\rangle$	$\langle e_7, 0.02, 0.04, 0.94\rangle$	$\langle e_8, 0.00, 0.01, 1.00\rangle$
A_4	$\langle e_1, 1.00, 0.01, 0.00\rangle$	$\langle e_2, 0.49, 0.07, 0.45\rangle$	$\langle e_3, 0.06, 0.04, 0.90\rangle$	$\langle e_4, 0.20, 0.04, 0.76\rangle$	$\langle e_5, 0.00, 0.01, 1.00\rangle$	$\langle e_6, 0.02, 0.01, 0.97\rangle$	$\langle e_7, 0.03, 0.03, 0.95\rangle$	$\langle e_8, 0.03, 0.03, 0.94\rangle$

Table 5: Fault diagnosis results based on the correlation coefficient of SNSs and SVM.

Fault type	Method	Test sample	Diagnosis result				Diagnosis accuracy rate (%)
			Healthy	Outer race fault	Ball fault	Inner race fault	
Healthy	SNSs	30	28		2		93.3
	SVM		27		3		90
Outer race fault	SNSs	30		28		2	93.3
	SVM			28		2	93.3
Ball fault	SNSs	30	5		25		83.3
	SVM		7		23		76.7
Inner race fault	SNSs	30				30	100
	SVM			5		25	83.3

4.5. Results and Discussions. To demonstrate the effectiveness of the new diagnosis method, we now provide two examples for fault diagnosis of bearings. Let us consider two testing bearing samples B_1 and B_2 described as neutrosophic sets:

$$\begin{aligned} B_1 = \{&\langle e_1, 1.00, 0.01, 0.00\rangle, \langle e_2, 0.51, 0.01, 0.49\rangle, \\ &\langle e_3, 0.08, 0.01, 0.92\rangle, \langle e_4, 0.24, 0.01, 0.76\rangle, \\ &\langle e_5, 0.00, 0.01, 1.00\rangle, \langle e_6, 0.03, 0.01, 0.97\rangle, \\ &\langle e_7, 0.05, 0.01, 0.95\rangle, \langle e_8, 0.06, 0.01, 0.94\rangle\}, \\ B_2 = \{&\langle e_1, 1.00, 0.01, 0.00\rangle, \langle e_2, 0.39, 0.01, 0.61\rangle, \\ &\langle e_3, 0.03, 0.01, 0.97\rangle, \langle e_4, 0.22, 0.01, 0.78\rangle, \\ &\langle e_5, 0.00, 0.01, 1.00\rangle, \langle e_6, 0.01, 0.01, 1.00\rangle, \\ &\langle e_7, 0.01, 0.01, 1.00\rangle, \langle e_8, 0.01, 0.01, 1.00\rangle\}. \end{aligned} \tag{20}$$

The correlation coefficient values between SNSs B_j ($j = 1, 2$) and A_k ($k = 1, 2, 3, 4$) can calculated by (17) as follows:

$$\begin{aligned} M_{\mathrm{SNS}}(A_1, B_1) &= 0.8787, \\ M_{\mathrm{SNS}}(A_2, B_1) &= 0.9483, \\ M_{\mathrm{SNS}}(A_3, B_1) &= 0.8746, \\ M_{\mathrm{SNS}}(A_4, B_1) &= 0.9819. \\ M_{\mathrm{SNS}}(A_1, B_2) &= 0.8587, \\ M_{\mathrm{SNS}}(A_2, B_2) &= 0.9714, \\ M_{\mathrm{SNS}}(A_3, B_2) &= 0.8566, \\ M_{\mathrm{SNS}}(A_4, B_2) &= 0.9590. \end{aligned} \tag{21}$$

For the fault-testing sample B_1, $M_{\mathrm{SNS}}(A_4, B_1)$ is the maximum correlation coefficient, and $M_{\mathrm{SNS}}(A_2, B_1)$ is the second correlation coefficient. According to the principle of correlation coefficient, the fault-diagnosis order is as follows:

$$A_4 \longrightarrow A_2 \longrightarrow A_1 \longrightarrow A_3. \tag{22}$$

Therefore, we can determine that the testing bearing is an inner race fault bearing. By actual observing, the testing bearing inner race was covered with scratches, and therefore the diagnosis result is correct.

Similarly, for the fault-testing sample B_2, the fault-diagnosis order is as follows:

$$A_2 \longrightarrow A_4 \longrightarrow A_1 \longrightarrow A_3. \tag{23}$$

By actual checking, the fault of the bearing firstly resulted from damage of outer race and then inner race. So the diagnosis results are consistent with the actual situation.

In the experiment, 120 rolling bearings were used for testing samples. In order to verify the effectiveness of the fault-diagnosis method proposed in this paper, we extracted the energy eigenvalues of bearing vibration signals firstly and then diagnosed the bearing faults using the correlation coefficient of SNSs and the support vector machine (SVM) [25], respectively. The fault-diagnosis results of rolling bearings are shown in Table 5. By comparing the diagnosis results shown in Table 5, it is clear that the diagnosis accuracy rate based on the correlation coefficient of SNSs is much higher than the accuracy rate based on SVM.

For further comparison, Table 6 lists the diagnosis results based on the correlation coefficient of SNSs, SVM, BP, and GA-BP [28] methods, respectively. Obviously, the method based on the correlation coefficient of SNSs can achieve the average accuracy rate of 92.5%, and it is higher than the ones based on the other methods.

The above comparisons demonstrate that the proposed method in this paper is effective in the bearing fault diagnosis.

5. Conclusion

To diagnose rolling bearing faults, a new fault-diagnosis method was developed by combining correlation coefficient of SNSs with wavelet packet decomposition. A series of experiments were conducted to diagnose rolling bearing faults, and the experimental results demonstrated that the proposed method can effectively identify the bearing faults. For the novel fault-diagnosis method, there exist two key issues: (1) extracting useful fault features by wavelet packet decomposition; (2) building the accurate SNSs models of bearing faults. In the future work, the two issues will be further improved based on the analysis of a large amount of

Table 6: Fault diagnosis results based on the correlation coefficient of SNSs, SVM, BP, and GA-BP.

Diagnosis method	Diagnosis accuracy rate (%)				Average accuracy (%)
	Healthy	Outer race fault	Ball fault	Inner race fault	
SNS	93.3	93.3	83.3	100	92.5
SVM	90	93.3	76.7	83.3	85.8
GA-BP	100	80	70	90	85
BP	90	70	50	90	75

experimental data since they will influence the accuracy of fault-diagnosis results.

Competing Interests

The author declares that there is no conflict of interests regarding the publication of this paper.

References

[1] A. S. Raj and N. Murali, "A novel application of Lucy-Richardson deconvolution: bearing fault diagnosis," *Journal of Vibration and Control*, vol. 21, no. 6, pp. 1055–1067, 2015.

[2] J. Lin and L. Qu, "Feature extraction based on morlet wavelet and its application for mechanical fault diagnosis," *Journal of Sound and Vibration*, vol. 234, no. 1, pp. 135–148, 2000.

[3] P. K. Kankar, S. C. Sharma, and S. P. Harsha, "Fault diagnosis of ball bearings using machine learning methods," *Expert Systems with Applications*, vol. 38, no. 3, pp. 1876–1886, 2011.

[4] D. H. Pandya, S. H. Upadhyay, and S. P. Harsha, "Fault diagnosis of rolling element bearing by using multinomial logistic regression and wavelet packet transform," *Soft Computing*, vol. 18, no. 2, pp. 255–266, 2014.

[5] R. Yan, M. Shan, J. Cui, and Y. Wu, "Mutual information-assisted wavelet function selection for enhanced rolling bearing fault diagnosis," *Shock and Vibration*, vol. 2015, Article ID 794921, 9 pages, 2015.

[6] P. H. Nguyen and J.-M. Kim, "Multifault diagnosis of rolling element bearings using a wavelet kurtogram and vector median-based feature analysis," *Shock and Vibration*, vol. 2015, Article ID 320508, 14 pages, 2015.

[7] C. Rajeswari, B. Sathiyabhama, S. Devendiran, and K. Manivannan, "Bearing fault diagnosis using wavelet packet transform, hybrid PSO and support vector machine," *Procedia Engineering*, vol. 97, pp. 1772–1783, 2014.

[8] B. Vishwash, P. S. Pai, N. Sriram, R. Ahmed, H. Kumar, and G. Vijay, "Multiscale slope feature extraction for gear and bearing fault diagnosis using wavelet transform," *Procedia Materials Science*, vol. 5, pp. 1650–1659, 2014.

[9] L.-Y. Zhao, L. Wang, and R.-Q. Yan, "Rolling bearing fault diagnosis based on wavelet packet decomposition and multiscale permutation entropy," *Entropy*, vol. 17, no. 9, pp. 6447–6461, 2015.

[10] P. Jayaswal, S. N. Verma, and A. K. Wadhwani, "Development of EBP-Artificial neural network expert system for rolling element bearing fault diagnosis," *Journal of Vibration and Control*, vol. 17, no. 8, pp. 1131–1148, 2011.

[11] L.-L. Jiang, H.-K. Yin, X.-J. Li, and S.-W. Tang, "Fault diagnosis of rotating machinery based on multisensor information fusion using SVM and time-domain features," *Shock and Vibration*, vol. 2014, Article ID 418178, 8 pages, 2014.

[12] A. Moosavian, H. Ahmadi, A. Tabatabaeefar, and M. Khazaee, "Comparison of two classifiers; K-nearest neighbor and artificial neural network, for fault diagnosis on a main engine journal-bearing," *Shock and Vibration*, vol. 20, no. 2, pp. 263–272, 2013.

[13] V. Sugumaran and K. I. Ramachandran, "Fault diagnosis of roller bearing using fuzzy classifier and histogram features with focus on automatic rule learning," *Expert Systems with Applications*, vol. 38, no. 5, pp. 4901–4907, 2011.

[14] W. Y. Liu and J. G. Han, "Rolling element bearing fault recognition approach based on fuzzy clustering bispectrum estimation," *Shock and Vibration*, vol. 20, no. 2, pp. 213–225, 2013.

[15] F. Harrouche and A. Felkaoui, "Automation of fault diagnosis of bearing by application of fuzzy inference system (FIS)," *Mechanics and Industry*, vol. 15, no. 6, pp. 477–485, 2014.

[16] L. A. Zadeh, "Fuzzy sets," *Information and Control*, vol. 8, no. 3, pp. 338–353, 1965.

[17] K. T. Atanassov, "Intuitionistic fuzzy sets," *Fuzzy Sets and Systems*, vol. 20, no. 1, pp. 87–96, 1986.

[18] K. Atanassov and G. Gargov, "Interval valued intuitionistic fuzzy sets," *Fuzzy Sets and Systems*, vol. 31, no. 3, pp. 343–349, 1989.

[19] F. Smarandache, *A Unifying Field in Logics, Neutrosophy: Neutrophic Probability, Set and Logic*, American Research Press, Rehoboth, Mass, USA, 1999.

[20] J. Ye, "Vector similarity measures of simplified neutrosophic sets and their application in multicriteria decision making," *International Journal of Fuzzy Systems*, vol. 16, no. 2, pp. 204–211, 2014.

[21] J. Ye, "Improved cosine similarity measures of simplified neutrosophic sets for medical diagnoses," *Artificial Intelligence in Medicine*, vol. 63, no. 3, pp. 171–179, 2015.

[22] A. Q. Ansari, R. Biswas, and S. Aggarwal, "Proposal for applicability of neutrosophic set theory in medical AI," *International Journal of Computer Applications*, vol. 27, no. 5, pp. 5–11, 2011.

[23] J. Ye, "Multicriteria decision-making method using the correlation coefficient under single-valued neutrosophic environment," *International Journal of General Systems*, vol. 42, no. 4, pp. 386–394, 2013.

[24] Y. Guo and H. D. Cheng, "New neutrosophic approach to image segmentation," *Pattern Recognition*, vol. 42, no. 5, pp. 587–595, 2009.

[25] Y. P. Sang, *Research on production test and intelligent diagnosis of rolling element bearing [M.S. thesis]*, China Jiliang University, 2015.

[26] R. Li, P. Sopon, and D. He, "Fault features extraction for bearing prognostics," *Journal of Intelligent Manufacturing*, vol. 23, no. 2, pp. 313–321, 2012.

[27] Y. Q. Wang, X. P. Wang, and L. C. Wang, "Pitch detection method based on morphological filtering," *Applied Mechanics and Materials*, vol. 596, pp. 433–436, 2014.

[28] B. S. Huang, W. Xu, and X. F. Zhou, "Rolling bearing diagnosis based on LMD and neural network," *International Journal of Computer Science*, vol. 10, no. 3, pp. 304–309, 2013.